

NACA RM L54D12a



RESEARCH MEMORANDUM

SUPERSONIC FLUTTER OF A 60° DELTA WING ENCOUNTERED DURING
THE FLIGHT TEST OF A ROCKET-PROPELLED MODEL

By William T. Lauten, Jr., and Joseph H. Judd

Langley Aeronautical Laboratory
Langley Field, Va.

CLASSIFICATION CHANGED

LIBRARY COPY

UNCLASSIFIED

JUN 22 1954

LANGLEY AERONAUTICAL LABORATORY
LIBRARY, NACA
LANGLEY FIELD, VIRGINIA

By authority of *Naca Res. Abs.* *4-8-57*
4 RN-114 Date *4-8-57*
NB 4-30-57

CLASSIFIED DOCUMENT

This material contains information affecting the National Defense of the United States within the meaning of the espionage laws, Title 18, U.S.C., Secs. 793 and 794, the transmission or revelation of which in any manner to an unauthorized person is prohibited by law.

NATIONAL ADVISORY COMMITTEE FOR AERONAUTICS

WASHINGTON

June 22, 1954

NATIONAL ADVISORY COMMITTEE FOR AERONAUTICS

RESEARCH MEMORANDUM

SUPERSONIC FLUTTER OF A 60° DELTA WING ENCOUNTERED DURING

THE FLIGHT TEST OF A ROCKET-PROPELLED MODEL

By William T. Lauten, Jr., and Joseph H. Judd

SUMMARY

An analysis of the flight time-history records of a rocket-propelled 60° delta-wing airplane configuration indicated that wing flutter started during the accelerating portion of the flight at a Mach number of approximately 1.7 and continued through the peak Mach number of the test ($M = 2.08$) and during deceleration at least until telemeter failure at $M = 1.4$ and probably to an even lower speed. CW Doppler velocimeter data indicated that the wings did not fail during the flight.

In order to document this case of flutter more fully, this being a primary purpose of this paper, the natural frequencies of vibration and the structural influence coefficients of the complete semispan wing, and the mass, moment of inertia, and center of gravity of streamwise strips were subsequently determined on a similar wing by laboratory tests.

The wing reported herein had the same plan form and airfoil section as a wing reported previously in NACA RM L52E06a but, because of the addition of surface inlays over the forward portion of the wing panel, was much stiffer and had much higher natural frequencies. This method of construction leaves the trailing edge and tip stiffnesses of the two wings approximately the same. A comparison of the flutter cases of these geometrically similar wings is of interest and indicates that, despite the differences in overall stiffness and frequency, the two wings fluttered over approximately the same speed range. This comparison shows that such a localized strengthening of the structure, although it might yield an increase in overall stiffness and natural frequencies, does not necessarily yield a significantly large increase in flutter speed.

INTRODUCTION

Recent developments in aircraft with delta wings have led to increased interest in flutter information concerning such plan forms. Although a considerable amount of experimental data on the aerodynamic characteristics of delta wings has been obtained over a wide range of Mach numbers (including the supersonic range) by the use of rocket-propelled models and by wind-tunnel tests, the amount of experimental flutter data is small. Some data on supersonic flutter of delta wings are presented in references 1, 2, and 3 and data on subsonic flutter are presented in reference 4.

As a part of an investigation of the zero-lift drag of airplane configurations with wing-mounted nacelles, a model having a 60° delta wing (NACA 65A003 airfoil section) was flight-tested without nacelles. During the flight of this configuration, a wing vibration identified as flutter started during the accelerating portion of the test flight just prior to booster separation, which occurred at a Mach number of approximately 1.7, and continued through the peak Mach number of the test ($M = 2.08$) and at least until the time at which the telemeter failed at a Mach number of 1.4. CW Doppler velocimeter data indicated that the wings did not fail during the flight.

The flutter data obtained during the flight test and the structural characteristics of a wing similar to the flight model are presented in this paper. Calculated mode shapes and frequencies are also presented. In addition, a comparison is made with a wing, reported in reference 1, which was identical in plan form and airfoil section and which fluttered over approximately the same Mach number range despite the fact that it was much weaker and had lower natural frequencies.

MODEL

Figure 1 presents a three-view drawing and figure 2 presents photographs of the flight model. The model was geometrically similar to the model of reference 1.

The wing used on the flight model had a 60° delta plan form with an NACA 65A003 airfoil section. A sheet of 0.091-inch 24S-T aluminum alloy with 0.030-inch maple veneer cycle-welded to each surface comprised the core. Spruce blocks, laid parallel to the wing leading edge, were glued to the core and cut to form the airfoil. In order to increase the stiffness of the wing, cutouts were made on the upper and lower surfaces and delta-shaped steel inlays 0.032 inch thick with 0.030-inch veneer cycle-welded on each side were glued into these cutouts. An

outline of the wing inlay may be seen in figure 3(a). The wing was constructed as a single panel which extended unbroken through the fuselage.

A 6.25-inch Deacon rocket motor booster was used to propel the flight model to supersonic speeds. The booster fins in the plane of the wing, as shown in figure 2(b), were 12.5 square feet in area. After separation of the model from the booster, a 3.25-inch aircraft rocket in the fuselage propelled the model to the peak Mach number. Weight and balance data for the model with and without rocket motor fuel are given in table I.

INSTRUMENTATION AND MEASUREMENTS

Flight Test

The data from the flight test were obtained by the use of telemeter, radiosonde, CW Doppler velocimeter, tracking radar, and cameras. Signals from the normal and longitudinal accelerometers of the model were transmitted and recorded by a telemeter system as the model traversed the speed range. Longitudinal location of the normal accelerometer is given in table I. Reduction of data from the radar units supplied time histories of velocity and flight path. A survey of atmospheric data for the test was made through radiosonde measurements from an ascending balloon.

Since the model had a high wing, a slight angle of attack was required for proper trim. The mean value of the normal accelerometer on the telemeter records was read and the normal-force coefficient for trim was computed. Over the Mach number range where telemeter data were obtained, the normal-force coefficient was approximately 0.006. Thus, the data presented in this report may be considered to be information at zero angle of attack.

Ground Tests

Since flutter was not anticipated during the flight test, the natural frequencies of the wing were not obtained. After the flight test, a similar half-wing was constructed for measurement of mass, vibration, and stiffness characteristics. A sketch of the wing showing the node lines for the first three modes of vibration and their associated frequencies are shown in figure 3(a). While the half-wing used in the laboratory tests could not be expected to be an exact duplicate of the wing tested in flight, the two were built from the same drawings so that quantities measured should be in good agreement for the two

wings. The data of figure 3(b) were included for convenience from reference 1 in order that the frequencies and node lines could be compared for wings with and without surface inlays.

Other quantities determined in the laboratory tests were the structural influence coefficients at twelve load points on the wing, the mass of the wing panels associated with these points, and the mass, moment of inertia (as determined by a bifilar suspension), and center of gravity of streamwise strips of the wing. The values of these properties are given in tables II, III, and IV. Figure 4 presents a sketch of the wing which shows the root restraint, points of load for influence coefficients, streamwise strips, and wing panels whose masses were determined for use with the structural influence coefficients. The load points were located at the intersection of the spanwise center line of the streamwise strips with the $16\frac{2}{3}$ -percent-chord, the 50-percent-chord, and the $83\frac{1}{3}$ -percent-chord lines. For convenience, each streamwise strip was divided into three equal parts measured along the spanwise center line of the strips. For the determination of the influence coefficients, the wing was loaded by means of a weighted frame which could be slipped over the wing in such a manner that a point load could be applied. The deflections were measured with dial gages which could be read directly to 10^{-4} inches.

The influence coefficients and the panel masses were used to form a dynamic matrix from which, by matrix iteration (ref. 5), the first three natural modes and their associated frequencies were calculated. These mode shapes and frequencies are tabulated in table V. In all three modes, the calculated frequencies, though somewhat lower, compare reasonably well with the values obtained experimentally. The mode shapes were not measured experimentally but the calculated node lines seem to be in reasonable agreement with the experimentally determined node lines.

RESULTS AND DISCUSSION

The telemeter record of the flight test showed oscillations of the normal accelerometer through part of the accelerating and decelerating flight. These oscillations are attributed to wing flutter. Because of the high longitudinal accelerations and the character of the normal forces encountered during the boost phase of the flight, the onset of flutter could not be definitely determined but large oscillations of the normal accelerometer started at a Mach number of approximately 1.7 and continued through the test peak Mach number of 2.08. The termination of flutter could not be determined either since the telemeter failed at Mach number 1.4 while the wing was still fluttering. However on the basis of the telemeter-record oscillations and previous experience, it

is felt that flutter continued into the transonic speed range. CW Doppler velocimeter data indicated that the wings did not fail in flight. The variation of Mach number, velocity, and density with time is shown in figure 5. Figure 6(a) presents the variation of flutter frequency with velocity. The flutter started just prior to separation of the model from the booster. The short period of coasting flight between separation from the booster and firing of the internal rocket motor is marked by scatter of the wing frequency data (indicated by flagged symbols on figure 6(a)). After rocket-motor firing, the frequency gradually decreased. The difference in slope of the frequency curve was attributed to the difference in longitudinal acceleration. This was about 20g during the accelerating flight, and varied from -7g to -3.5g during decelerating flight.

It is of interest to make a comparison between the two geometrically similar wings, the wing reported in reference 1 and the wing reported herein. The primary difference was that the second wing had set into its upper and lower surfaces a delta-shaped steel sheet which greatly increased the stiffness and natural frequencies. The differences in frequencies may be seen by comparing figures 3(a) and 3(b) which show the node lines for the first three modes of vibration and their associated natural frequencies. The outline of the steel sheet may be seen in figure 3(a). It is evident that the change in construction would not affect appreciably the stiffness of the wing in the region of the tip and trailing edge. In figures 6(a) and 6(b), there is shown the frequency spectrum for the two wings. The ratios of the first to third natural frequencies for each wing were approximately the same, 0.327 for the unstiffened wing and 0.346 for the wing with the steel plates.

The behavior of the wings was somewhat similar in regard to flutter frequency. The initial frequency in both tests was near the third mode and in both cases the frequency decreased. However, for the unstiffened wing there was a sudden shift in frequency near a velocity of 1,890 ft/sec (Mach number of 1.7) indicating a change in the flutter mode. No such shift is apparent in the behavior of the stiffened wing.

Since the telemeter failed for the wing reported herein, the cessation of flutter cannot be determined but, presumably, it is within one- or two-tenths of the Mach number of the unstiffened wing reported in reference 1. This shows that a particular localized strengthening of the structure, such as that accomplished on this wing by plates laid into the surface, will not necessarily yield a significantly large increase in flutter speed, although it might yield an increase in the overall stiffness and in the natural frequencies. On the other hand, it is quite possible that a smaller increase in overall stiffness might yield a significant increase in flutter speed if some other section of the wing panel were stiffened or if the stiffness was increased by a more efficient method.

CONCLUDING REMARKS

A comparison with the wing reported in NACA RM L52E06a shows that the wing reported herein, which had the same geometry but different construction, had much higher natural frequencies and was much stiffer, except in the region of the tip and trailing edge, than the wing reported previously and further shows that the two wings fluttered over approximately the same Mach number range. This leads to the conclusion that a localized strengthening of the structure as reported herein, although it might yield an increase in the overall stiffness and in the natural frequencies, will not necessarily yield a significantly large increase in flutter speed.

Langley Aeronautical Laboratory,
National Advisory Committee for Aeronautics,
Langley Field, Va., March 26, 1954.

REFERENCES

1. Judd, Joseph H., and Lauten, William T., Jr.: Flutter of a 60° Delta Wing (NACA 65A003 Airfoil) Encountered at Supersonic Speeds During the Flight Test of a Rocket-Propelled Model. NACA RM L52E06a, 1952.
2. Lauten, William T., Jr., and Mitcham, Grady L.: Note on Flutter of a 60° Delta Wing Encountered at Low-Supersonic Speeds During the Flight of a Rocket-Propelled Model. NACA RM L51B28, 1951.
3. Tuovila, W. J.: Some Wind-Tunnel Results of an Investigation of the Flutter of Sweptback- and Triangular-Wing Models at Mach Number 1.3. NACA RM L52C13, 1952.
4. Herr, Robert W.: A Preliminary Wind-Tunnel Investigation of Flutter Characteristics of Delta Wings. NACA RM L52B14a, 1952.
5. Scanlan, Robert H., and Rosenbaum, Robert: Introduction to the Study of Aircraft Vibration and Flutter. The MacMillan Co., 1951.

TABLE I.- WEIGHT AND BALANCE DATA FOR FLIGHT MODEL

Model with rocket fuel:	
Weight, lb	70.25
Wing loading, lb/sq ft	16.70
Center-of-gravity position, in.	43.00
Model without rocket fuel:	
Weight, lb	60.00
Wing loading, lb/sq ft	14.25
Center-of-gravity position, in.	42.87
Normal-accelerometer position, in.	40.35

TABLE II.- STRUCTURAL INFLUENCE COEFFICIENTS AT LOAD POINTS SHOWN IN FIGURE 4

[25-pound load]

Load points	Deflection, in inches, at load points -											
	1	2	3	4	5	6	7	8	9	10	11	12
1	0.3080	0.0257	0.0041	0.0003	0.3417	0.0638	0.0087	0.0013	0.3552	0.0930	0.0127	0.0015
2	.0265	.0172	.0035	.0004	.0249	.0144	.0054	.0014	.0235	.0128	.0053	.0010
3	.0041	.0035	.0035	.0004	.0040	.0031	.0021	.0010	.0038	.0026	.0013	.0003
4	.0002	.0004	.0004	.0009	.0004	.0004	.0003	.0001	.0004	.0002	.0001	.0001
5	.3423	.0250	.0035	.0003	.4275	.0666	.0088	.0015	.4509	.1175	.0177	.0020
6	.0636	.0141	.0030	.0003	.0689	.0294	.0061	.0012	.0739	.0376	.0105	.0016
7	.0091	.0058	.0020	.0002	.0094	.0065	.0038	.0008	.0107	.0067	.0039	.0008
8	.0016	.0013	.0007	.0000	.0017	.0013	.0010	.0007	.0015	.0012	.0008	.0001
9	.3554	.0242	.0033	.0004	.4517	.0727	.0093	.0015	.2103	.1418	.0198	.0023
10	.0926	.0128	.0024	.0002	.1167	.0370	.0065	.0011	.1401	.0891	.0217	.0026
11	.0126	.0055	.0015	.0001	.0159	.0102	.0036	.0007	.0194	.0219	.0210	.0032
12	.0018	.0010	.0003	.0000	.0019	.0017	.0008	.0002	.0024	.0027	.0033	.0037

TABLE III.- MASS OF NUMBERED PANELS OF WING SHOWN IN FIGURE 4

Panel designation (see fig. 4)	Mass, slugs
1	0.00196
2	.00737
3	.01942
4	.03137
5	.00122
6	.00619
7	.02508
8	.04159
9	.00089
10	.00415
11	.00846
12	.01730
<i>total</i>	<i>.16500</i>

TABLE IV.- PROPERTIES OF STREAMWISE STRIPS OF WING SHOWN IN FIGURE 4

Streamwise strip	Spanwise extent of strip, in. from wing root	Center of gravity, in. from L.E. along center line of strip	Mass, slugs	Mass polar moment of inertia, in.-lb-sec ²
I	0 to 4	10.80	0.0895	0.2902
II	4 to 8	7.58	.0526	.0816
III	8 to 12	4.70	.0177	.0173
IV	12 to tip	1.30	.0040	.0010

TABLE V.- FREQUENCIES AND CALCULATED MODE SHAPES

Load points (see fig. 4)	1st mode (1st bending)	2nd mode (2nd bending)	3rd mode (1st torsion)
1	0.8387	-0.7992	0.5314
2	.0863	.4045	.7438
3	.0165	.1448	.2918
4	.0016	.0265	.0665
5	1.0000	-1.0000	-.1220
6	.2082	.4930	.2609
7	.0365	.2508	.2940
8	.0069	.0627	.0963
9	.9396	-.4902	-.2775
10	.3521	.9208	-1.0000
11	.0694	.6834	-.2699
12	.0100	.1307	-.0098
Calculated frequency, cps	65.7	146.7	204
Experimental frequency, cps	71.5	160	207

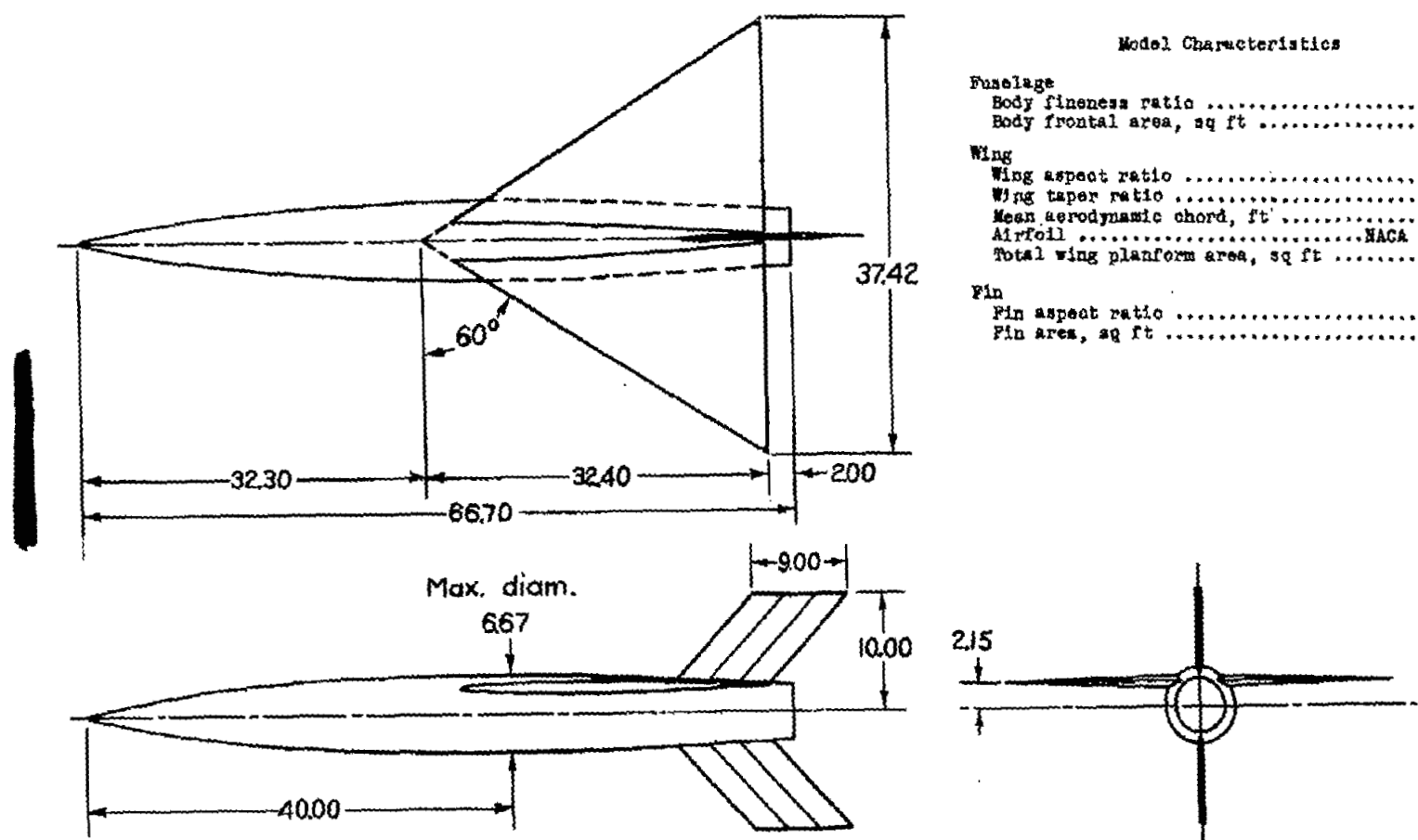
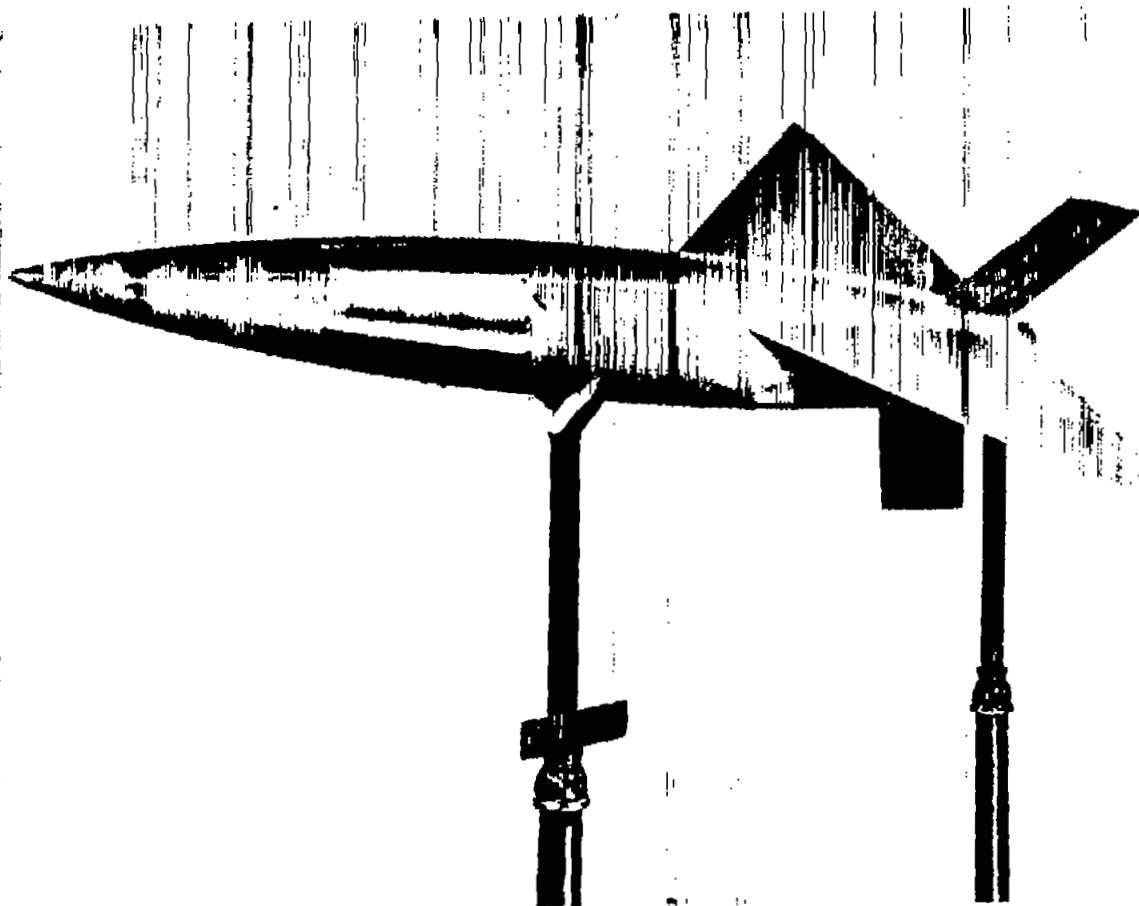


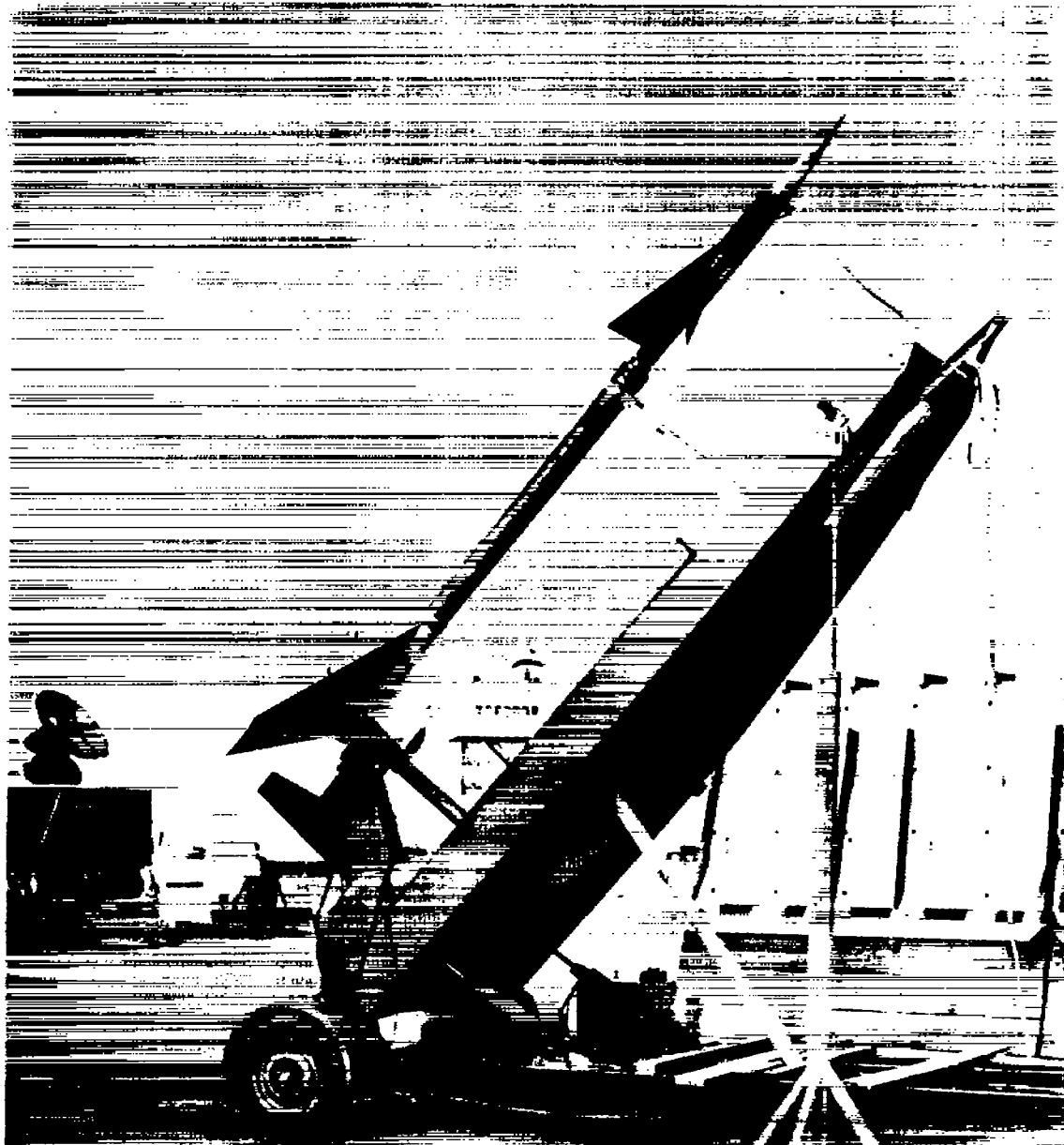
Figure 1.- Three-view drawing of the rocket-powered flight model. All dimensions in inches.



L-78531.1

(a) Flight model.

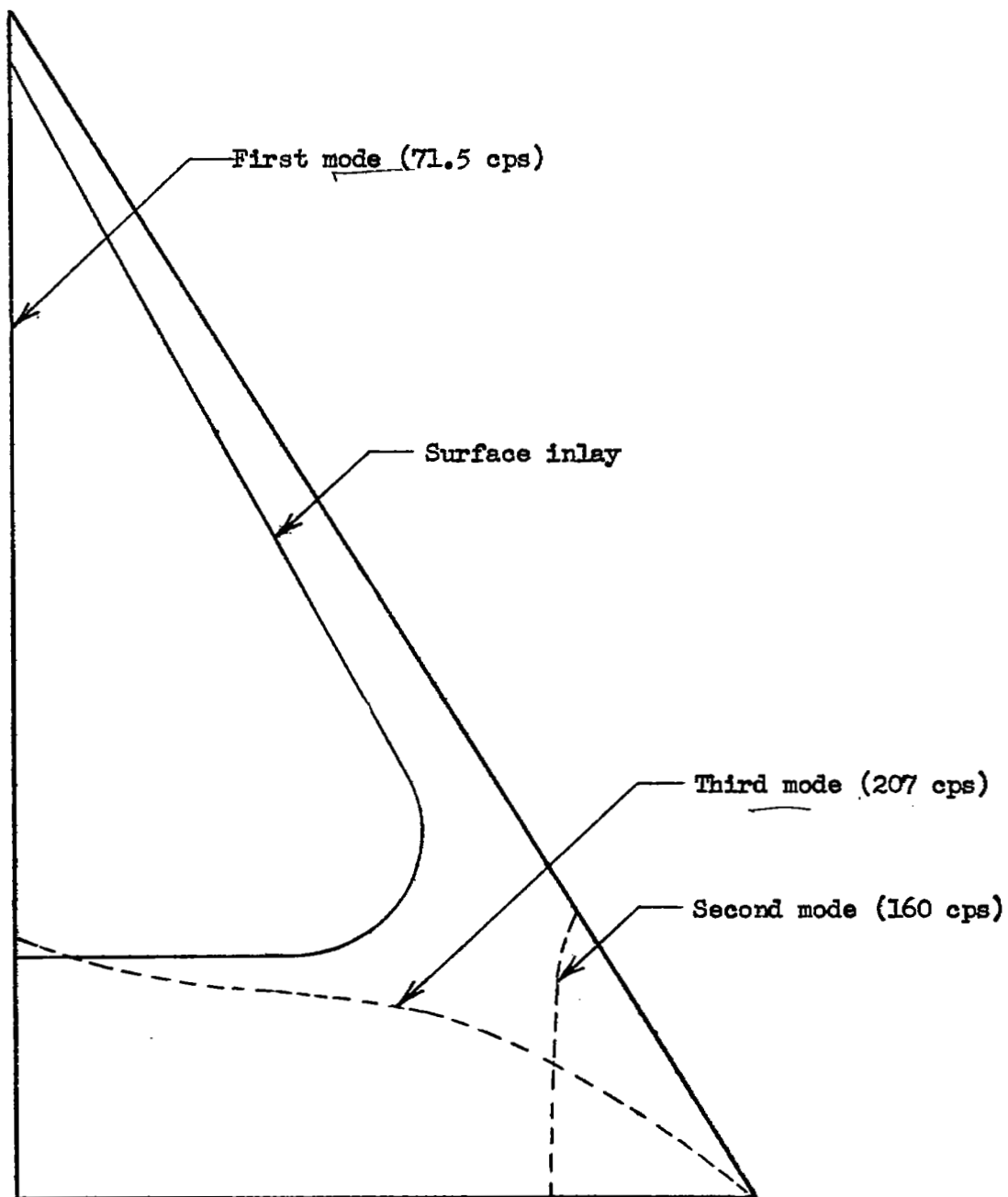
Figure 2.- Photographs of flight model.



(b) Model and booster prior to flight.

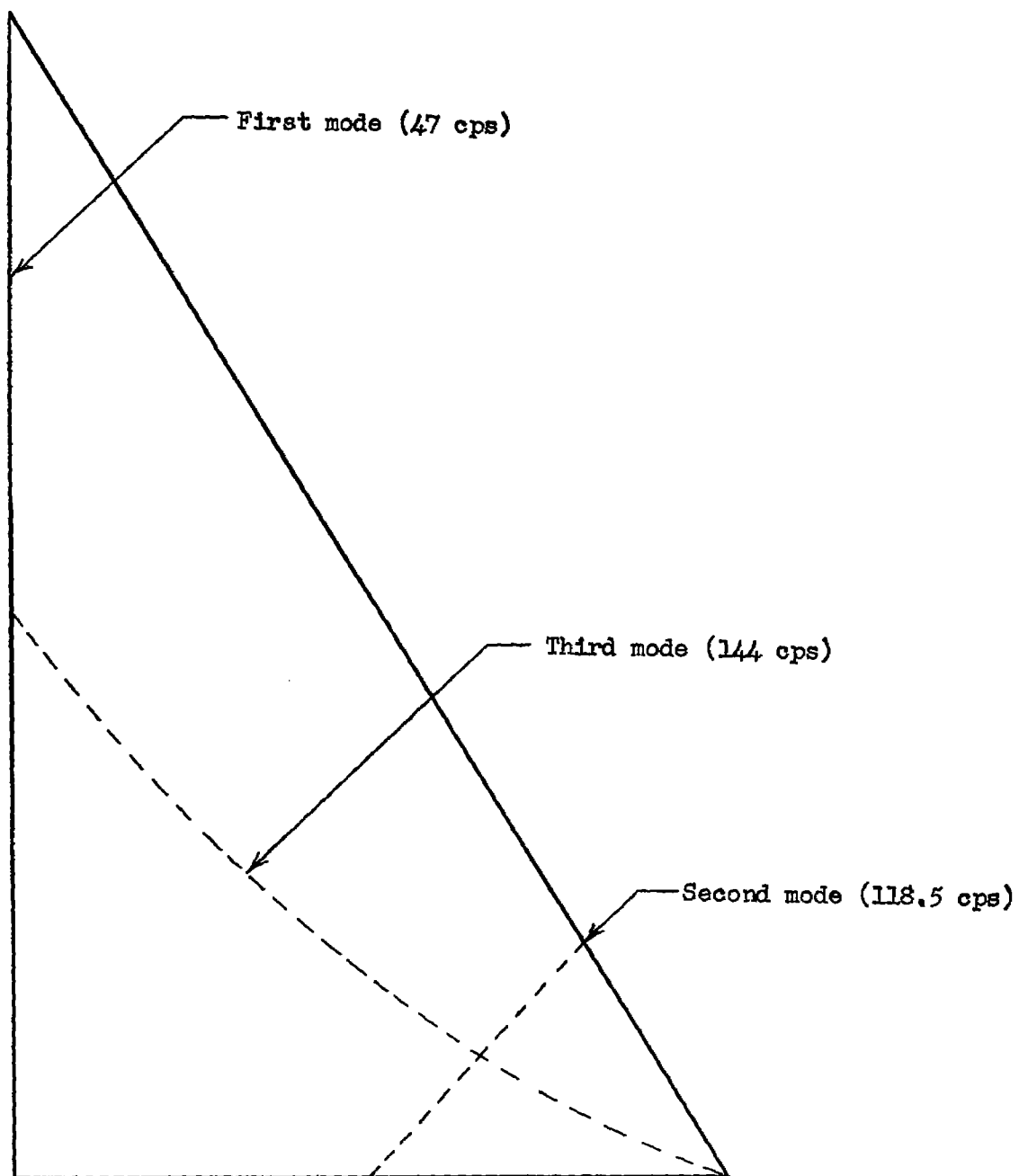
L-79041.1

Figure 2.- Concluded.



(a) With surface inlay.

Figure 3.- Sketch of half-wing showing node lines and frequencies of vibration.



(b) Without surface inlay.

Figure 3.- Concluded.

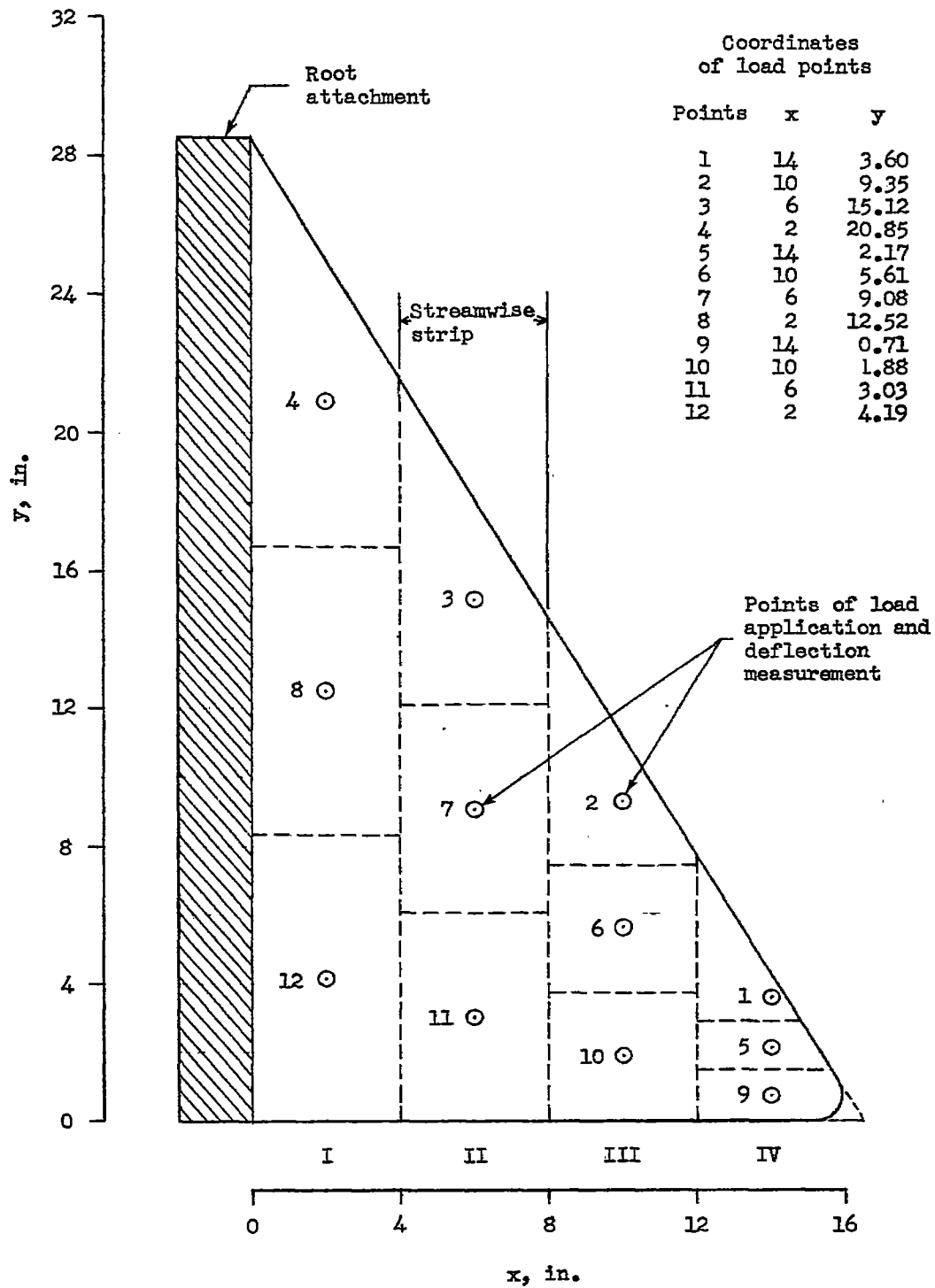


Figure 4.- Schematic drawing of ground-test wing showing points of load application and deflection measurement.

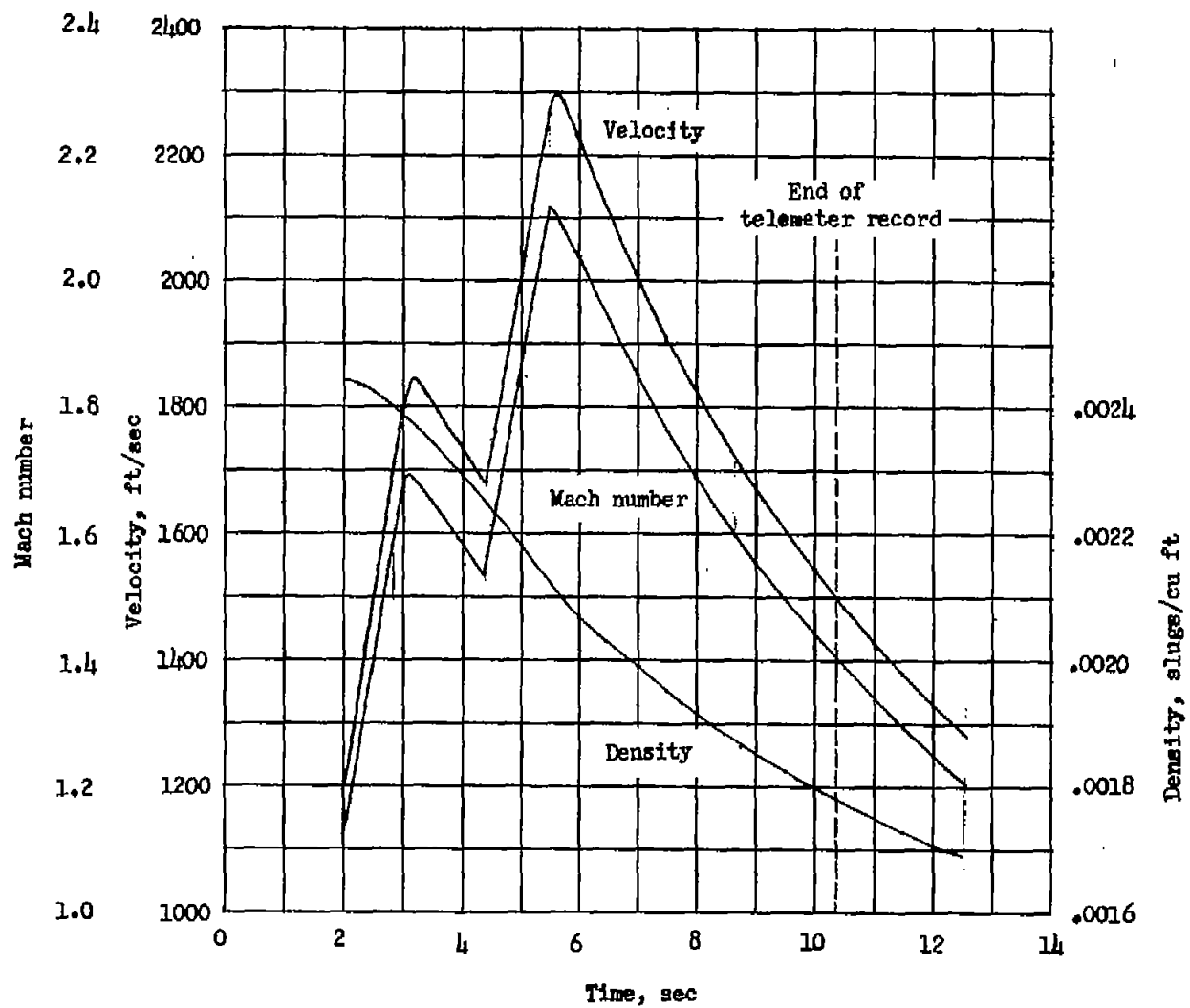
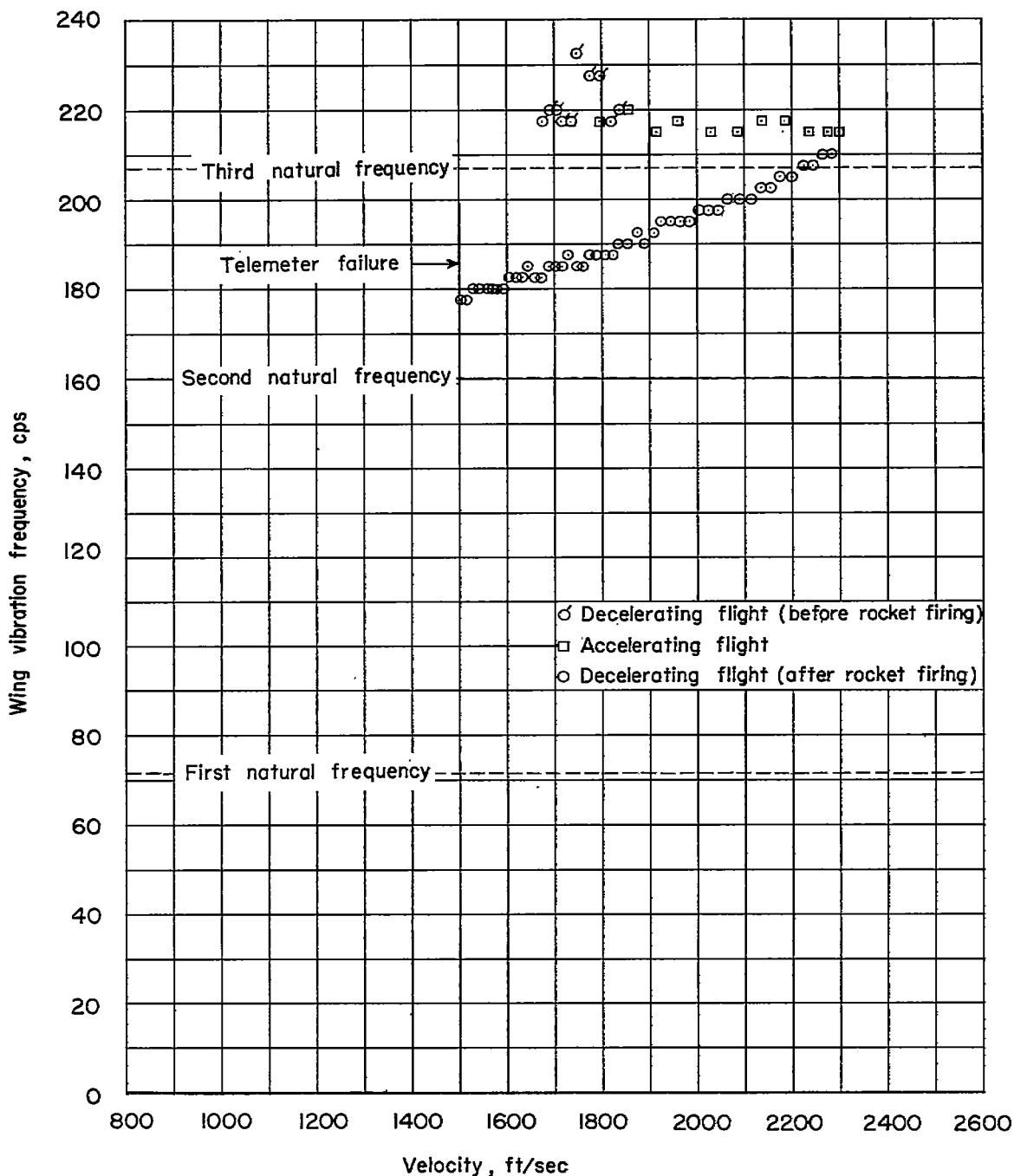
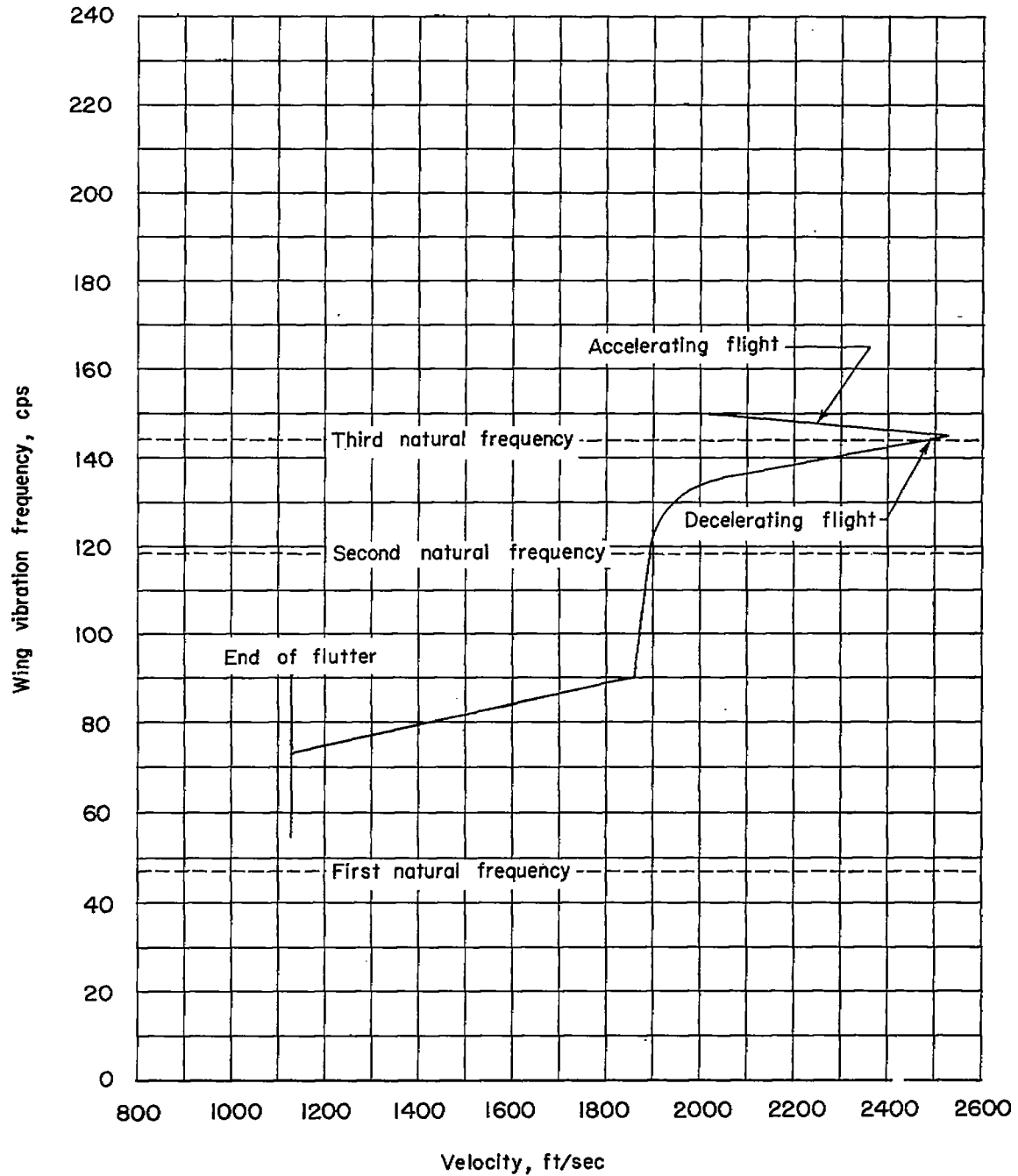


Figure 5.- Variation of Mach number, velocity, and density with time for a portion of the rocket-model flight.



(a) Wing with steel inlay.

Figure 6.- Variation of wing frequency with model velocity.



(b) Unstiffened wing (ref. 1).

Figure 6.- Concluded.